

Subject-specific strength percentile determination for two-dimensional symmetric lifting considering dynamic joint strength

Received: 24 November 2017 / Accepted: 14 December 2018 / Published online: 3 January 2019 © Springer Nature B.V. 2019

Abstract This paper describes an efficient optimization method for determining the subjectspecific strength percentile and predicting the maximum weight lifting motion by considering dynamic joint strength in symmetric box lifting. Dynamic strength is modeled as a three-dimensional function of joint angle and joint angular velocity based on experimentally obtained joint strength data from the literature. The function is further formulated as the joint torque limit constraint in an inverse dynamics optimization formulation to predict the maximum weight lifting motion. The initial, mid-time, and final postures are obtained from experiments and imposed as tracking constraints in the optimization formulation. In addition, the box weight and time duration are given as inputs for the lifting optimization problem. The normalized joint torque squared is used as the objective function. Subjectspecific strength percentile (z score) is enumerated until the optimal solution is achieved. The determined strength percentile is a global score considering interactions of all joints for the two-dimensional symmetric lifting task. Results show that incorporating dynamic strength is critical in predicting lifting motion in extreme lifting conditions. The proposed algorithm can determine the subject-specific strength percentile based on experimental box lifting data. The accurate strength percentile is critical to predict strength related tasks to protect workers from injury.

Keywords Lifting · Dynamic joint strength · Strength percentile · Maximum weight · Inverse dynamics optimization · Motion prediction · Manual material handling

1 Introduction

Manual material handling, particularly lifting, poses an injury risk to many workers and is considered a major cause of work-related low back pain and impairment. Lifting is a

✓ Y. Xiang yujiang.xiang@okstate.edu

Department of Mechanical Engineering, Texas Tech University, Lubbock, TX 79409, USA



School of Mechanical and Aerospace Engineering, Oklahoma State University, Stillwater, OK 74078, USA

dynamic process and each body joint for the worker is bounded by its dynamic joint strength to ensure the lifting task is achieved without any injury. Dynamic joint strength can be modeled as a three-dimensional function of joint angle and joint angular velocity, which are functions of time. Thus, dynamic joint strength is an implicit function of time which is more accurate than the constant static strength values in human modeling. For heavy box lifting, the joint strength percentile estimation to adapt the joint load to the worker is important for individual's injury prevention.

The dynamic strengths for particular joints could be modeled by using experimental data for a set of subjects [1–4]. The dynamic joint strength needs to be scaled when applied to an individual. However, it is difficult to determine the subject-specific strength percentile (z_score) which is required for a dynamic simulation. In this study, we formulate the two-dimensional (2D) symmetric maximum weight lifting as a dynamic optimization problem. The maximum box weight, time duration, initial, mid-time, and final postures are given as inputs for the dynamic lifting optimization formulation. The optimization is carried out by sequentially increasing z_score value until the optimization algorithm converges. The corresponding strength percentile is the subject-specific strength percentile for the symmetric maximum weight lifting. This strength percentile is a global score for all joints considering their interactions for the task.

For the last few decades, researchers developed biomechanical prediction approaches for lifting. Compared with the experimental method of using human subjects to assess problems during lifting, biomechanical models can provide relatively new alternative technologies that allow direct testing and subject-specific results. In addition, it is risky to use human subjects to determine the maximum weight-lifting motion. On the other hand, the experimental and simulation methods are complimentary, and the simulation model needs to be validated by experiments before application [5, 6]. Dynamic motion optimization algorithms can predict different strategies for lifting using different objective functions and set of constraints [7-12]. Lifting motion prediction is essentially an optimal control problem. The motion is generated using certain optimization principles with given boundary conditions. The direct optimization method transfers the optimal control problem into a nonlinear programming (NLP) problem [13]. For optimization-based motion predictions, there are different optimization formulations, such as forward dynamics optimization [14, 15], inverse dynamics optimization [16-19], and optimization with direct collocation [20, 21]. Another prediction tool for lifting is the well-known NIOSH lifting equation which is an index based method and it cannot describe the details of dynamic lifting process.

For human motion predictions, constraints are critical in predicting accurate human motions. Some physical constraints, such as joint angle limits and joint torque limits, must be enforced throughout motion. Many simulations reported in the literature used static strength for approximation [10–12, 16–19, 21]. Dynamic joint strength has been experimentally tested and reported in the literature [1–4, 22, 23], but only a few have been used in simulation to predict more accurate human motion, such as reported in Farizeh and Sadigh [24] who studied a fast-walking problem. Therefore, it is important to use dynamic strength instead of static strength for motion prediction under extreme conditions. This paper reports an efficient optimization method to determine the subject-specific strength percentile in a symmetric maximum weight box-lifting task. The ultimate goal is to develop a subject-specific and real-time ergonomic tool to protect workers from injury for both symmetric and asymmetric lifting tasks.



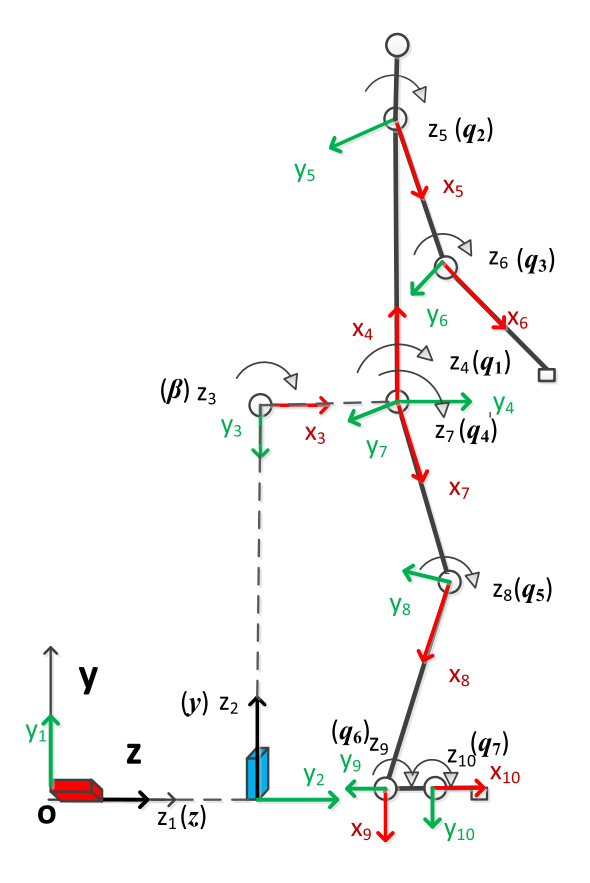
2 Method

2.1 Human skeletal model

A 2D skeletal model with 10 degrees of freedom (DOF) defined in joint space is used to simulate symmetric lifting motion, as shown in Fig. 1. Three DOF are used for global translation (y, z) and rotation (β) , and seven DOF (q_1, q_2, \ldots, q_7) are used for the body joints. The global DOF are composed of two translational (prismatic) joints and one rotational (revolute) joint. The anthropometric data for the skeletal model is generated using GEBOD® software based on experimental data.

Figure 1 depicts how the DOF are set up in the Denavit–Hartenberg (DH) method [25]. The degree of freedom is given in the local z-direction in both the translational joint and the rotational joint. Note that the global rotation joint (z_3) , spine joint (z_4) , and hip joint (z_7) coincide at the same location. The positive directions for all the rotation joints $(z_3 - z_{10})$ are clockwise in the global Y-Z plane. There are two branches in the body frame with respect to the global coordinate branch (parent): the spine–arm branch and leg branch. In the spine–arm branch, two arms are represented as a single branch, since only 2D symmetric lifting is studied. The arm branch includes upper arm and lower arm. In the leg branch, two legs are combined as a single branch including thigh, tibia, and foot. The DH parameters, θ , d, a, α , [25] are described in Table 1.

Fig. 1 The 2D lifting skeletal model





Tuble 1 Diff table for a 2D framati model										
DOF (Positive direction)	θ	d	а	α	Segment					
z (Forward translation)	π	0	0	$\pi/2$	Global translation					
y (Upward translation)	$\pi/2$	Leg length	0	$-\pi/2$						
β (Clock-wise rotation)	0	0	0	0	Global rotation					
q_1 (Spine flexion)	$-\pi/2$	0	Spine length	0	Spine					
q_2 (Shoulder flexion)	π	0	Upper arm length	0	Arm					
q_3 (Elbow extension)	0	0	Lower arm length	0						
q_4 (Hip extension)	$\pi/2$	0	Thigh length	0	Leg					
q ₅ (Knee flexion)	0	0	Tibia length	0						
q ₆ (Ankle plantar flexion)	$-\pi/2$	0	Hinder foot length	0						
az (Metatarsophalangeal extension)	0	0	Fore foot length	0						

Table 1 DH table for a 2D human model

The kinematics and dynamics are calculated using the DH-based recursive Lagrangian approach [26]. The EOM is expressed in Eqs. (1)–(5), where the first term in the torque expression (Eq. (1)) is the inertia and Coriolis torque, the second term is the torque due to gravity load, the third term is the torque due to external force, and the fourth term represents the torque due to the external moment:

$$\tau_{i} = \operatorname{tr}\left(\frac{\partial A_{i}}{\partial q_{i}}\mathbf{D}_{i}\right) - \mathbf{g}^{\mathrm{T}}\frac{\partial \mathbf{A}_{i}}{\partial q_{i}}\mathbf{E}_{i} - \mathbf{f}_{k}^{\mathrm{T}}\frac{\partial \mathbf{A}_{i}}{\partial q_{i}}\mathbf{F}_{i} - \mathbf{G}_{i}^{\mathrm{T}}\mathbf{A}_{i-1}\mathbf{z}_{0},\tag{1}$$

$$\mathbf{D}_{i} = \mathbf{I}_{i} \mathbf{C}_{i}^{\mathrm{T}} + \mathbf{T}_{i+1} \mathbf{D}_{i+1}, \tag{2}$$

$$\mathbf{E}_i = m_i \mathbf{r}_i + \mathbf{T}_{i+1} \mathbf{E}_{i+1},\tag{3}$$

$$\mathbf{F}_i = \mathbf{r}_k \delta_{ik} + \mathbf{T}_{i+1} \mathbf{F}_{i+1},\tag{4}$$

$$\mathbf{G}_i = \mathbf{h}_k \delta_{ik} + \mathbf{G}_{i+1},\tag{5}$$

where $\operatorname{tr}(\cdot)$ is the trace of a matrix, \mathbf{A}_i and \mathbf{C}_i are the recursive kinematics position and acceleration matrices, respectively, q_i is the joint angle, \mathbf{I}_i is the inertia matrix for link i, \mathbf{D}_i is the recursive inertia and Coriolis matrix, \mathbf{g} is the gravity vector, m_i is the mass of link i, \mathbf{r}_i is the center of mass of link i, $\mathbf{f}_k = [0 \ f_{ky} \ f_{kz} \ 0]^T$ is the external force applied on link k, \mathbf{r}_k is the position of the external force in the local frame k, $\mathbf{h}_k = [h_x \ 0 \ 0 \ 0]^T$ is the external moment applied on link k, \mathbf{T}_i is the link transformation matrix, $\mathbf{z}_0 = [0 \ 0 \ 1 \ 0]^T$ is for a revolute joint, $\mathbf{z}_0 = [0 \ 0 \ 0 \ 0]^T$ is for a prismatic joint, and δ_{ik} is Kronecker delta. The detailed derivations of \mathbf{A}_i and \mathbf{C}_i are described in [26, 27].

2.2 Maximum weight lifting experiments

A maximum load lifting study was conducted with 23 healthy males split into three age categories at Texas Tech University with the approved IRB. Fifteen were in the 20–30 years of age category, five in the 31–45 and three in the 50–60. The male subjects studied covered all different stature percentiles and had a low BMI. Three dimensional kinematic data was collected at 100 Hz using Vicon Nexus motion capture system (VICON, Oxford, UK). Five cameras were placed around the room with one in each corner and one in the front middle of the room. A plug-in-gait model with added iliac crests, giving 42 markers total, was used for the marker protocol [28]. There were two force plates, one under each of the subject's feet, which collected ground reaction forces (GRF) at 2000 Hz. Electromyographic (EMG)



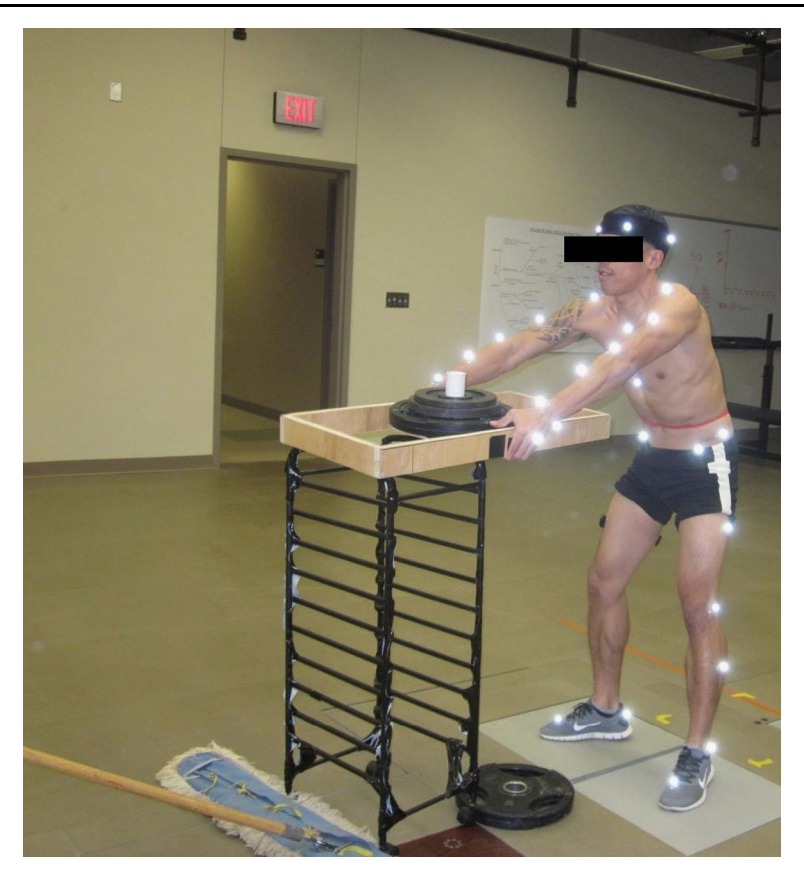


Fig. 2 Maximum weight lifting experiment

Trigno system (Delsys, Inc., Natick, MA, USA) was put on the following muscles; external oblique, internal oblique, rectus femoris, latissimus dorsi, erector spinae, multifidus, glutaeus maximus, and medial hamstring. Symmetry was assumed so only the right side muscle activity was collected. The EMG data was also collected at 2000 Hz. The following anthropometric measurements were taken for each subject: height, weight, leg length, ankle width, knee width, wrist width, elbow width, shoulder offset, inter-asis distance, and waist circumference [29, 30].

For the lifting study, each participant was asked to psychophysically determine their maximum weight lifting capability. The entire maximum was not used to avoid injury during the experiment. Once the weight was determined, the lifting study was initiated. The subject was asked to lift three different sized boxes in three directions with three trials for each lifting which gave a total of 27 lifts. A randomized table was created to avoid any learning curve. The three directions for lifting were symmetric (forwards) and asymmetric (left and right). The three sizes of the box were small (35 cm \times 35 cm \times 15 cm), medium (50 cm \times 35 cm \times 15 cm), and large (65 cm \times 35 cm \times 15 cm). As the box did not have handles, it was placed in front of the subject on top of a weight about 2.54 cm off the floor so the subject could fit their fingers beneath the box. The subject then lifted the box in the most comfortable and natural way and set it down on a 1 meter tall table that was either in front of them or to their side, as seen in Fig. 2. Following the experiment, the data was processed in the



motion capture software Vicon Nexus. All markers were labeled and the data was smoothed and converted into a C3D file. That C3D file was then used in Visual 3D (C-Motion, Inc., Germantown, MD, USA). A skeletal model was created following the marker protocol used in the experiments. This skeletal model consisted of 15 segments and was used to output coordinates, joint angles, and joint moments. The anthropometric measurements taken for each subject were used to create distinct and accurate skeletal models allowing for more precise calculations.

In this paper we extract experimental data for 2D symmetric lifting and 19 out of 23 subjects are used for this study (sex, male; age, 30.58 ± 11.45 years; height, 180.8 ± 6.2 cm; body mass, 82.17 ± 11.87 kg, where \pm indicates standard deviation). The other four subjects' motion capture data were found incomplete and therefore discarded.

2.3 Dynamic joint strength

As reported in the literature [1–4], the dynamic isokinetic and isometric strengths of ankle, knee, hip, spine, shoulder, and elbow were tested using experiments through a normal range of motion. The peak torque for a given joint position and angular velocity was measured. These data can be used to model joint dynamic strength surface as a function of joint angle and angular velocity. In this section, a surrogate model is developed from the experimental data. The logistic equations are used to model the peak torque as a function of both joint angle and angular velocity, and the coefficients of the logistic function are obtained from Gauss least squares regressions. The corresponding peak torque-angle-velocity relationship is given as:

$$\tau_{\text{peak_U}}^{i} = c_{1} + c_{2} \frac{4e^{-(q_{i}-c_{3})/c_{4}}}{[1 + e^{-(q_{i}-c_{3})/c_{4}}]^{2}} + c_{5} \frac{4e^{-(v_{i}-c_{6})/c_{7}}}{[1 + e^{-(v_{i}-c_{6})/c_{7}}]^{2}}
+ c_{8} \frac{4e^{-(q_{i}-c_{3})/c_{4}}}{[1 + e^{-(q_{i}-c_{3})/c_{4}}]^{2}} \frac{4e^{-(v_{i}-c_{6})/c_{7}}}{[1 + e^{-(v_{i}-c_{6})/c_{7}}]^{2}},$$
(6a)
$$\tau_{\text{peak_L}}^{i} = c_{1} + c_{2} \frac{4e^{-(q_{i}-c_{3})/c_{4}}}{[1 + e^{-(q_{i}-c_{3})/c_{4}}]^{2}} + c_{5} \frac{4e^{-(v_{i}-c_{6})/c_{7}}}{[1 + e^{-(v_{i}-c_{6})/c_{7}}]^{2}}
+ c_{8} \frac{4e^{-(q_{i}-c_{3})/c_{4}}}{[1 + e^{-(q_{i}-c_{3})/c_{4}}]^{2}} \frac{4e^{-(v_{i}-c_{6})/c_{7}}}{[1 + e^{-(v_{i}-c_{6})/c_{7}}]^{2}},$$
(6b)

where $c_1 \sim c_8$ are regression equation coefficients, e is the exponential function, q_i is the ith joint angle, $v_i = \dot{q}_i$ is the ith joint angular velocity, $\tau^i_{\text{peak_U}}$ is the upper peak torque value for the ith joint in positive q_i direction, and $\tau^i_{\text{peak_L}}$ is the lower peak torque value for the ith joint in negative q_i direction.

The coefficients in Eqs. (6a), (6b) are scaled mean values, and along with the coefficient covariance (CV) determined with each curve fit. Therefore, a specific percentile strength can be determined as follows:

$$\tau_{\text{peak_U}}^{i_p\%} = z_\text{score} * \text{CV}_{\text{U}}^{i} * \tau_{\text{peak_U}}^{i} + \tau_{\text{peak_U}}^{i}, \tag{7a}$$

$$\tau_{\text{peak_L}}^{i_p\%} = z_\text{score} * \text{CV}_{\text{L}}^{i} * \tau_{\text{peak_L}}^{i} + \tau_{\text{peak_L}}^{i}, \tag{7b}$$

where $au_{\mathrm{peak_U}}^{i_p\%}$ is the pth percentile upper torque limit for the ith joint, and $au_{\mathrm{peak_L}}^{i_p\%}$ is the pth percentile lower torque limit for the ith joint; both $au_{\mathrm{peak_L}}^{i_p\%}$ and $au_{\mathrm{peak_L}}^{i_p\%}$ are calculated from same $z_$ score. There is one-to-one relationship between the pth percentile and $z_$ score.



We modeled dynamic strengths for ankle, knee, hip, spine, shoulder, and elbow joints, using experimental data from the literature [1–4]. In Eqs. (7a), (7b), $\tau_{\text{peak_U}}^i$, $\tau_{\text{peak_L}}^i$, CV_{U}^i , and CV_{L}^i are statistical values obtained from experiments. However, it is difficult to determine the subject-specific strength percentile (z_score) which is required for a dynamic simulation. In this study, we formulate the maximum weight lifting as a dynamic optimization problem. The upper and lower peak torque values in Eqs. (7a), (7b) are used in joint torque constraints and objective function. The maximum box weight, time duration, initial, mid-time, and final postures are given as inputs for the dynamic lifting optimization problem. The optimization is carried out by sequentially increasing z_score value until the optimization algorithm converges. The corresponding strength percentile is the subject-specific global strength percentile for the maximum weight lifting.

2.4 Symmetric lifting motion prediction formulation

2.4.1 Objective function

For lifting motion, the design variables are the optimal control points P of joint angle profiles. The normalized dynamics effort is used as an objective function for the lifting motion, which is defined as time integration of all normalized joint torque squared [16–18]:

$$J(\mathbf{P}) = \sum_{i=4}^{\text{ndof}} \int_0^T \left(\frac{\tau_i(\mathbf{P})}{\tau_{\text{peak_U}}^{i-p\%}(t) - \tau_{\text{peak_L}}^{i-p\%}(t)} \right)^2 dt, \tag{8}$$

where ndof is the number of DOF. Note that the joint torque for each global DOF is zero for a balanced lifting motion.

2.4.2 Constraints

The general constraints for a 2D symmetric lifting motion include:

(1) Joint angle limits

$$\mathbf{q}^{\mathrm{L}} \le \mathbf{q}(t) \le \mathbf{q}^{\mathrm{U}},\tag{9}$$

where \mathbf{q}^{L} is the lower joint angle limit and \mathbf{q}^{U} is the upper limit;

(2) Joint torque limits

$$0 \le \frac{\tau_i(t) - \tau_{\text{peak_L}}^{i_- p_{\text{eak_L}}}(t)}{\tau_{\text{peak_U}}^{i_- p_{\text{eak_U}}}(t) - \tau_{\text{peak_L}}^{i_- p_{\text{eak_L}}}(t)} \le 1;$$
(10)

(3) Feet contacting positions

$$P(\text{feet}, t) = P_{\text{feet}}^{s},\tag{11}$$

where P_{feet}^{s} is the specified feet contact position on level ground;

(4) Balance condition

$$P(ZMP, t) \in FSR,$$
 (12)

where the zero moment point (ZMP) position is inside the foot support region (FSR);



(5) Collision avoidance

$$d(t) \ge r_1 + r_2,\tag{13}$$

where d is the calculated distance between the hand and the circle center on the body segment representing the body thickness, r_1 is half of the box width, and r_2 is the radius of the circle. Seven circles are filled into body segments: two for spine and five for leg;

(6) Initial and final hand positions

$$P(\text{hand}, t = 0, T) = P_{\text{hand}}^{s}(t = 0, T),$$
 (14)

where P_{hand}^{s} is the specified hand position at initial and final times;

(7) Initial and final velocities

$$\dot{\mathbf{q}}(t=0,T) = \mathbf{0},\tag{15}$$

where the initial and final lifting motions are static;

(8) Initial and final postures

$$\left|\mathbf{q}(t) - \mathbf{q}^{s}(t)\right| \le \varepsilon, \quad t = 0, \frac{T}{2}, T,$$
 (16)

where \mathbf{q}^s is the specified experimental posture, and $\varepsilon = 0.1$.

All these constraints and optimization algorithm are described in detail in [10, 11, 31]. Joint trajectory is interpolated by using B-splines with five control points for each joint. There are 50 design variables and 523 nonlinear constraints for the symmetric lifting motion optimization. The dynamic strengths of all joints are considered in the optimization. The initial guess for design variables is $\mathbf{P} = \mathbf{0}$. The SQP-based optimizer, SNOPT [32], is used to solve the optimization problem. The optimal solution is obtained in 4.43 seconds CPU time on average on a laptop with Intel® Core i5-7200U @ 2.50 GHz, 2.70 GHz, and 8 GB RAM.

3 Results

Simulation results for all 19 subjects' symmetric maximum weight box liftings are conducted and compared with the experimental data. The subject's initial, mid-time, final postures, box weight, and total lifting time are all specified in the simulation as shown in Table 2. The motions between the initial and final postures are predicted by using the optimization formulation in Sect. 2.4. The minimum *z*_score and the corresponding strength percentile for each subject to ensure the optimization converges are shown in Table 2.

The stick diagrams of the predicted maximum weight lifting motions are depicted in Fig. 3. A representative subject (#5) is chosen to show the predicted joint angles, vertical GRF, and joint torques in Figs. 4, 5, and 6, respectively.

4 Discussion

In Fig. 3, most subjects use a perfect squat lifting strategy with large ankle dorsi-flexion and knee flexion, and small spine flexion at initial posture. In contrast, Subjects 1, 9, 13, and 14 use a combined squat and back lifting strategy with large spine and knee flexion at initial



Table 2 Maximum weight box lifting input parameters, z_score, and global strength percentile

Subject #	Initial y* (m)	Final y (m)	Initial z* (m)	Final z (m)	Weight (N)	Time (s)	z_score	Percentile %
1	0.070	0.980	0.428	0.323	343.98	1.36	1.63	94.84
2	0.101	1.090	0.424	0.540	233.73	1.65	0.47	68.08
3	0.102	1.069	0.444	0.461	189.63	1.77	-0.07	47.21
4	0.107	1.047	0.483	0.437	255.78	1.80	0.30	61.79
5	0.070	1.088	0.418	0.417	233.73	1.44	0.69	75.49
6	0.088	1.091	0.449	0.487	211.68	1.93	0.21	58.32
7	0.057	1.144	0.450	0.581	233.73	1.55	0.68	75.17
8	0.077	1.106	0.514	0.424	233.73	1.41	1.16	87.70
9	0.081	0.989	0.444	0.347	145.53	1.54	-0.25	40.13
10	0.050	1.170	0.528	0.480	233.73	2.17	0.76	77.64
11	0.078	1.037	0.543	0.362	255.78	1.41	0.86	80.51
12	0.084	1.210	0.492	0.493	233.73	1.59	0.43	66.64
13	0.086	1.143	0.463	0.378	211.68	2.06	0.39	65.17
14	0.075	1.118	0.480	0.491	145.53	1.57	0.23	59.10
15	0.067	1.098	0.393	0.394	167.58	1.57	0.06	52.39
16	0.053	1.098	0.483	0.384	211.68	2.40	0.61	72.91
17	0.096	1.203	0.457	0.480	211.68	1.70	0.31	62.17
18	0.074	1.139	0.475	0.528	211.68	1.36	0.73	76.73
19	0.094	0.994	0.397	0.336	277.83	1.21	0.86	80.51

^{*}Note that y is the vertical height measured from hand to ground, and z is the horizontal distance measured from hand to ankle

posture. This may be a subject-specific strategy and may not be optimal for the maximum weight lifting. In this case, the predicted strength percentile will underestimate the subject's strength. If the subject is trained properly, he/she could lift more weight.

For the maximum weight lifting of Subject 5, we can see that hip dynamic strength is activated in Fig. 6(d). Hip joint strength is activated for almost one-third of time period at the beginning stage of lifting. Spine is close to be activated in the middle of lifting (Fig. 6(a)); other joints are not activated. In addition, the upper dynamic hip strength value is time dependent and less than the static strength value. These illustrate the importance of imposing dynamic joint strength for maximum weight lifting compared to using static joint strength. These also demonstrate the hip and spine are critical joints in maximum weight lifting.

In this study, we use posture constraints to track the experimental data for the simulation similar to [33]. We allow $\varepsilon=0.1$ rad for each joint angle difference between the simulation and experimental data at the initial, mid-time, and final postures. The advantage of this method is that only *one parameter* ε is adjusted for tracking the experimental data. The smaller value of ε gives more accurate tracking results, which further refines the predicted strength percentile. However, it is more difficult for the optimization problem to converge during simulation. Therefore, to determine an appropriate ε value, we need to balance the accuracy and convergence of the simulation for all 19 subjects. Although, adding a tracking term in the objective function can also make the simulation and experiment have similar trends, tuning the weighting coefficients is not trivial and can significantly affect the predicted results. In addition, the combined objective functions partially represent the cen-



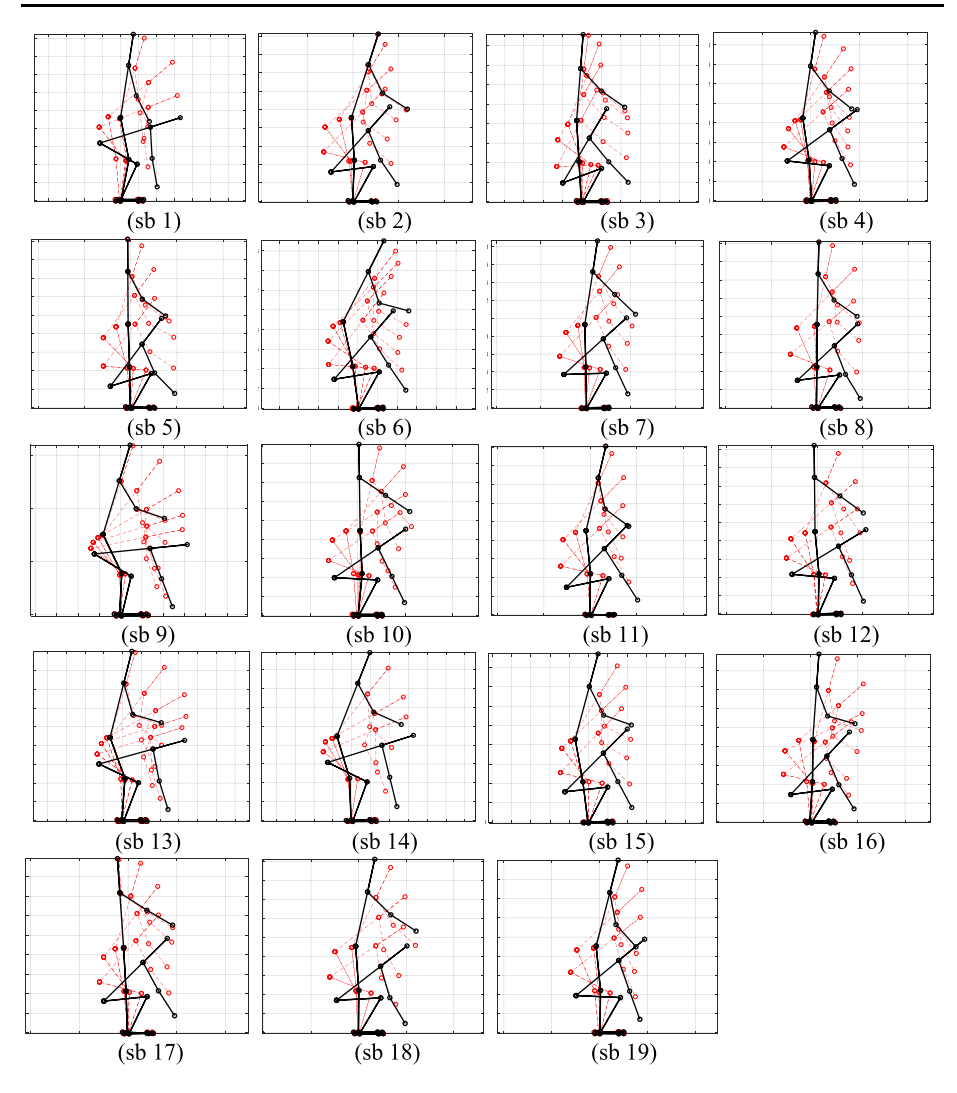


Fig. 3 Snapshots of all 19 subjects' maximum weight lifting motions (sb, subject index)

tral nervous system. Therefore, the objective function tracking technique is not used in this study. The general trends of the simulation results are matching well with the experimental data as shown in Figs. 4 and 5.

Due to the various sources for the experimental data, expressed in various ways, and collected on a large range of subjects [1, 2, 4], there are some errors in the dynamic strength database. The model needs several precautions whenever it is implemented, but this is beyond the scope of our study. Recently, Frey-Law's group has extended the dynamic strength data to all joints [3, 4]. Anderson et al. [34] also studied peak torque value as a function of joint angle and angular velocity for the lower extremity. However, only a few subjects were used to collect data and the interaction between the torque-angle and torque-velocity was not studied.



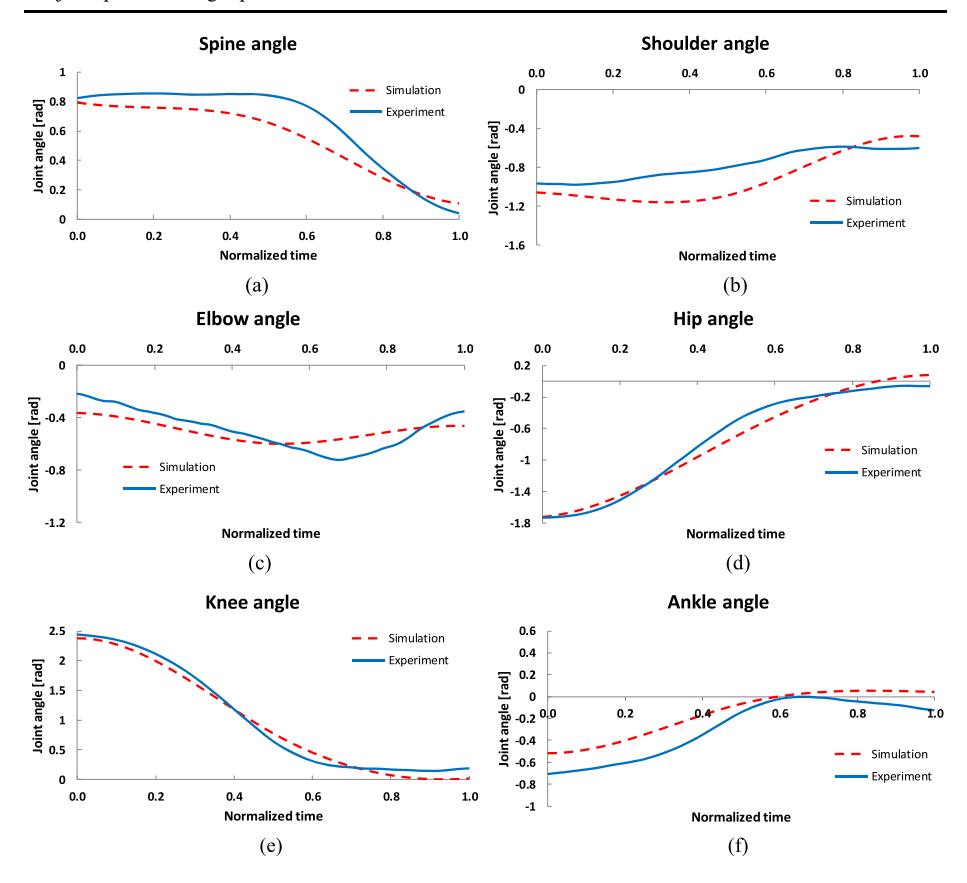
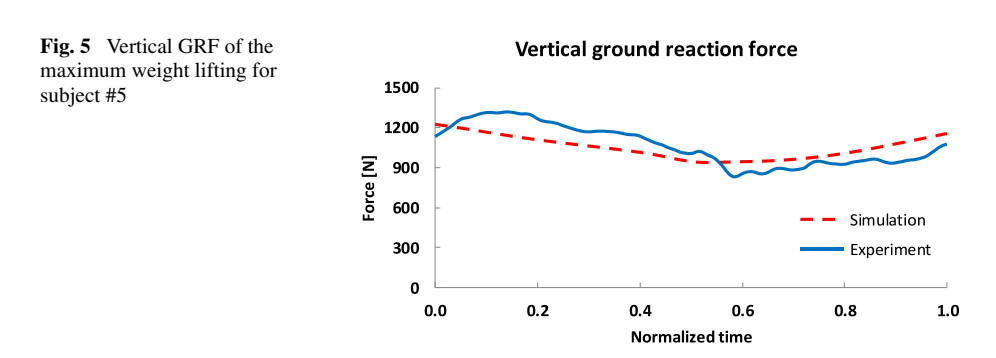


Fig. 4 Joint angle profiles of the maximum weight lifting for subject #5: (a) spine, (b) shoulder, (c) elbow, (d) hip, (e) knee, and (f) ankle



In this study, the symmetric lifting motion is simulated using an inverse dynamics optimization method. The dynamic joint strengths are modeled using experimental data, and incorporated in the optimization formulation to predict the maximum lifting motions and subject-specific strength percentiles. For a lifting task, the initial, mid-time and final postures, box weight, and total time are imposed as constraints in the optimization formulation. The *z*_score is sequentially enumerated to increase the strength limits to make the maximum



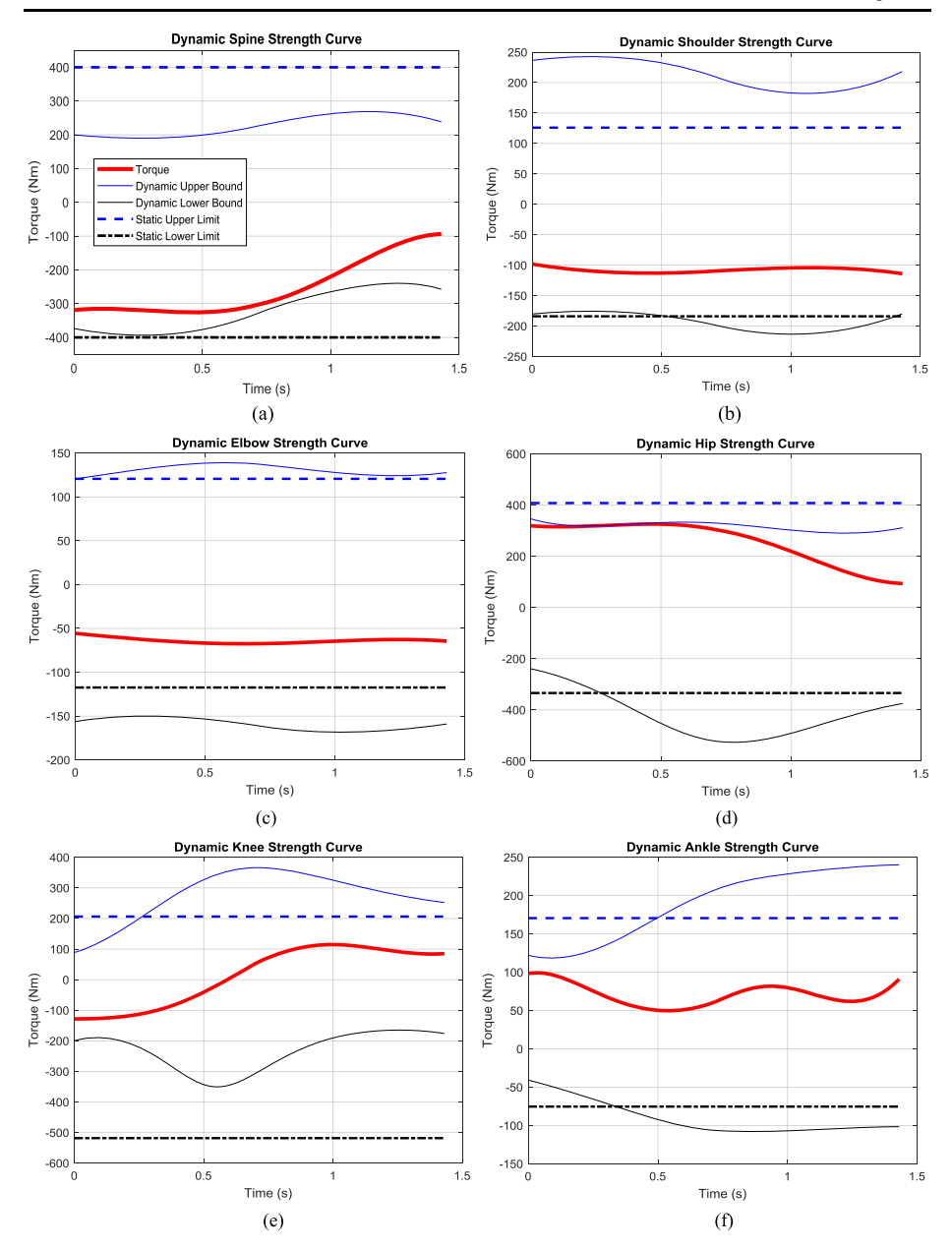


Fig. 6 Joint torque profiles of the maximum weight lifting for subject #5: (a) spine, (b) shoulder, (c) elbow, (d) hip, (e) knee, and (f) ankle

weight lifting optimization converge. Furthermore, the obtained *z*_score value is the global strength percentile for the subject. It is noted that the global score represents all joints for a particular task. People may have clear discrepancies for upper and lower limb strength, and also for different tasks. The global strength score is a task based concept considering the interactions of all joints, which is different from the joint by joint isokinetic strength test. Each



of the 19 subjects' strength percentiles is predicted. These subject-specific strength values are critical to predict other strength related tasks to protect them from injury in manual material handling. Future work includes (1) whole body dynamic strength model implementation; (2) extension of this 2D model to 3D to study asymmetric lifting.

Acknowledgements This research is supported by projects from NSF (Award #1700865, 1849279, and 1703093).

Publisher's Note Springer Nature remains neutral with regard to jurisdictional claims in published maps and institutional affiliations.

References

- Stockdale, A.A.: Modeling three-dimensional hip and trunk peak torque as a function of joint angle and velocity. Ph.D. thesis, Department of Biomedical Engineering, The University of Iowa, Iowa City, IA (2011)
- Frey-Law, L.A., Laake, A., Avin, K.G., Heitsman, J., Marler, T., Abdel-Malek, K.: Knee and elbow 3D strength surfaces: peak torque-angle-velocity relationships. J. Appl. Biomech. 28(6), 726-737 (2012)
- Looft, J.M.: Adaptation and validation of an analytical localized muscle fatigue model for workplace tasks. Ph.D. thesis, Department of Biomedical Engineering, The University of Iowa, Iowa City, IA (2014)
- Hussain, S.J., Frey-Law, L.A.: 3D strength surfaces for ankle plantar- and dorsi-flexion in healthy adults: an isometric and isokinetic dynamometry study. J. Foot Ankle Res. 9(43), 1–10 (2016)
- Freivalds, A., Chaffin, D.B., Garg, A., Lee, K.S.: A dynamic biomechanical evaluation of lifting maximum acceptable loads. J. Biomech. 17(4), 251–262 (1984)
- Zhang, X., Nussbaum, M.A., Chaffin, D.B.: Back lift versus leg lift: an index and visualization of dynamic lifting strategies. J. Biomech. 33(6), 777–782 (2000)
- 7. Ayoub, M.M.: Problems and solutions in manual materials handling—the state-of-the-art. Ergonomics **35**(7–8), 713–728 (1992)
- Huang, C., Sheth, P.N., Granata, K.P.: Multibody dynamics integrated with muscle models and spacetime constraints for optimization of lifting movements. In: ASME IDETC/CIE Conference, September 24–28, 2005, Long Beach, California (2005)
- 9. Arisumi, H., Chardonnet, J.R., Kheddar, A., Yokoi, K.: Dynamic lifting motion of humanoid robots. In: IEEE International Conference on Robotics and Automation, Roma, Italy, pp. 2661–2667 (2007)
- Xiang, Y., Arora, J.S., Rahmatalla, S., Marler, T., Bhatt, R., Abdel-Malek, K.: Human lifting simulation using a multi-objective optimization approach. Multibody Syst. Dyn. 23(4), 431–451 (2010)
- Xiang, Y., Arora, J.S., Abdel-Malek, K.: 3D human lifting motion prediction with different performance measures. Int. J. Humanoid Robot. 9(02), 1250012 (2012)
- Song, J., Qu, X., Chen, C.H.: Simulation of lifting motions using a novel multi-objective optimization approach. Int. J. Ind. Ergon. 53, 37–47 (2016)
- 13. Xiang, Y., Arora, J.S., Abdel-Malek, K.: Physics-based modeling and simulation of human walking: a review of optimization-based and other approaches. Struct. Multidiscip. Optim. **42**(1), 1–23 (2010)
- Thelen, D.G., Anderson, F.C.: Using computed muscle control to generate forward dynamic simulations of human walking from experimental data. J. Biomech. 39(6), 1107–1115 (2006)
- Shourijeh, M.S., McPhee, J.: Forward dynamic optimization of human gait simulations: a global parameterization approach. J. Comput. Nonlinear Dyn. 9, 031018 (2014)
- Fregly, B.J., Reinbolt, J.A., Rooney, K.L., Mitchell, K.H., Chmielewski, T.L.: Design of patient-specific gait modifications for knee osteoarthritis rehabilitation. IEEE Trans. Biomed. Eng. 54(9), 1687–1695 (2007)
- Ren, L., Jones, R.K., Howard, D.: Predictive modelling of human walking over a complete gait cycle. J. Biomech. 40(7), 1567–1574 (2007)
- Xiang, Y., Arora, J.S., Rahmatalla, S., Abdel-Malek, K.: Optimization-based dynamic human walking prediction: one step formulation. Int. J. Numer. Methods Eng. 79(6), 667–695 (2009)
- Farahani, S.D., Andersen, M.S., de Zee, M., Rasmussen, J.: Optimization-based dynamic prediction of kinematic and kinetic patterns for a human vertical jump from a squatting position. Multibody Syst. Dyn. 36(1), 37–65 (2016)
- Arora, J.S., Wang, Q.: Review of formulations for structural and mechanical system optimization. Struct. Multidiscip. Optim. 30(4), 251–272 (2005)



 Ackermann, M., van den Bogert, A.J.: Optimality principles for model-based prediction of human gait. J. Biomech. 43(6), 1055–1060 (2010)

- Cahalan, T.D., Johnson, M.E., Liu, S., Chao, E.Y.: Quantitative measurements of hip strength in different age-groups. Clin. Orthop. Relat. Res. 246, 136–145 (1989)
- Kumar, S.: Isolated planar trunk strengths measurement in normal: Part III—results and database. Int. J. Ind. Ergon. 17(2), 103–111 (1996)
- Farizeh, T., Sadigh, M.J.: A mathematical framework to study fast walking of human. Multibody Syst. Dyn. 40(2), 99–122 (2017)
- Denavit, J., Hartenberg, R.S.: A kinematic notation for lower-pair mechanisms based on matrices. ASME J. Appl. Mech. 22, 215–221 (1955)
- Xiang, Y., Arora, J.S., Abdel-Malek, K.: Optimization-based motion prediction of mechanical systems: sensitivity analysis. Struct. Multidiscip. Optim. 37(6), 595–608 (2009)
- Toogood, R.W.: Efficient robot inverse and direct dynamics algorithms using micro-computer based symbolic generation. IEEE Int. Conf. Robot. Autom. 3, 1827–1832 (1989)
- Cloutier, A., Boothby, R., Yang, J.: Motion capture experiments for validating optimization-based human models. In: HCI International, 3rd International Conference on Digital Human Modelling, July 9–14, 2011, Florida, USA (2011)
- Mital, A., Kromodihardjo, S.: Kinetic analysis of manual lifting activities: Part I—Development of a three-dimensional computer model. Int. J. Ind. Ergon. 1, 77–101 (1986)
- Schultz, A., Andersson, G., Ortengren, R., Haderspeck, K., Nachemson, A.: Loads on the lumbar spine. Validation of a biomechanical analysis by measurements of intradiscal pressures and myoelectric signals. J. Bone Jt. Surg. 64(5), 713–720 (1982)
- Kim, J.H., Xiang, Y., Yang, J., Arora, J.S., Abdel-Malek, K.: Dynamic motion planning of overarm throw for a biped human multibody system. Multibody Syst. Dyn. 24(1), 1–24 (2010)
- Gill, P.E., Murray, W., Saunders, M.A.: SNOPT: an SQP algorithm for large-scale constrained optimization. SIAM J. Optim. 12(4), 979–1006 (2002)
- Xiang, Y., Arora, J.S., Abdel-Malek, K.: Hybrid predictive dynamics: a new approach to simulate human motion. Multibody Syst. Dyn. 28(3), 199–224 (2012)
- 34. Anderson, D.E., Madigan, M.L., Nussbaum, M.A.: Maximum voluntary joint torque as a function of joint angle and angular velocity: model development and application to the lower limb. J. Biomech. **40**(14), 3105–3113 (2007)

